Journal of Energy Storage 50 (2022) 104488

Contents lists available at ScienceDirect

Journal of Energy Storage

journal homepage: www.elsevier.com/locate/est

Research papers

Efficient temperature estimation for thermally stratified storage tanks with buoyancy and mixing effects

Ana Soares [a,b,*,1], Juliano Camargo [c,d], Jad Al-Koussa [c,d], Jan Diriken [c,d], Johan Van Bael [c,d], Jesus Lago [c,d,e]

[a] INESC Coimbra, DEEC, Rua Sílvio Lima, Pólo II, Coimbra 3030-290, Portugal
[b] Department of Electrical and Computer Engineering, University of Coimbra, Rua Sílvio Lima, Polo II, 3030-290, Coimbra, Portugal
[c] EnergyVille, Thor Park 8310, Genk, Belgium
[d] Energy Technology, Flemish Institute for Technological Research (VITO), Mol, Belgium
[e] Delft Center for Systems and Control, Delft University of Technology, Delft, The Netherlands

ARTICLE INFO

Keywords:
State estimation
Stratified thermal energy storage tank
1-dimensional model
Parameter estimation

ABSTRACT

Estimating the state thermal storage devices is key to use them efficiently to reduce the uncertainty of renewable sources. Although stratified storage tanks are one of the most efficient and cost-effective storage systems, they lack accurate state estimation methods. In this paper, we propose a general methodology for estimating the state of thermally stratified storage tanks of different topologies and capacity. The method is based on a simple moving horizon estimation technique and a 1-D smooth model that can integrate buoyancy effects into a smooth equation. The novelty of the proposed approach is that it is the first state estimation approach that considers both buoyancy and mixing effects. This distinction is paramount to an adequate estimation of the temperature distribution in the storage tank which can then be used for different aims, namely as a basis for model predictive controls. Besides the novel state estimation approach, the paper has three more contributions: (i) it shows how a model for seasonal storage devices can be further extended to smaller stratified tanks with different topologies; (ii) it modifies such a model so that the model equations can be integrated into a single dynamical equation; (iii) it proposes the most complete case study to date for modeling and estimating temperature distribution inside small stratified storage tanks. The analysis of the proposed approach is done in several stages. First, to validate the applicability of the model to small tanks and multiple topologies, we perform a model identification and parameter estimation for three different stratified tanks. Second, we test the accuracy of the proposed state estimation approach in those three stratified tanks employing the estimated parameters in the first experimental study and the models also previously defined. Finally, to further validate the models, we perform a simulation for each of the three tanks and we compare the accuracy of the simulation against real data. As we show, both the state estimation approach and the model are satisfactorily accurate as they display average mean errors below 2 °C.

1. Introduction

The increasing share of renewables in the energy system has put a lot of attention on technologies and methods which can help minimizing the impact of renewables intermittency and balance the differences between generation and demand [1–5]. According to [5], the mitigation of the impact of renewables intermittency and uncertainty can be done through:

- aggregation of supply, demand, and reserves using transmission interconnections;
- storage technologies, both thermal and electrical;
- flexible generation and conversion;
- energy demand flexibility; and
- other demand-side mechanisms.

To optimize the use of thermal energy storage technologies, like sensible heat storage water tanks, and to adequately design suitable control strategies, namely when to charge and discharge the tanks, state estimation, in case of inexistence of enough temperature sensors or in case of failure of any of them, is crucial. State estimation, as defined in

* Corresponding author.
E-mail address: ana.soares@inescc.pt (A. Soares).
[1] Ana Soares was previously with Vito/EnergyVille.

https://doi.org/10.1016/j.est.2022.104488
Received 2 October 2020; Received in revised form 17 March 2022; Accepted 18 March 2022
Available online 14 April 2022

the context of this paper, is an indicator giving information about the temperature distribution of the water inside the thermal storage units in face of certain conditions which might change over time. This indicator can then be used in different applications, namely at the industrial and residential sectors. Under this scenario, the temperature distribution estimated could be used in combination with minimum and maximum temperature thresholds to calculate the state of charge (SoC) of a tank. The SoC would thus be defined in this perspective as the ratio of the energy content of the water compliant to the requirements set by the users, versus the reference energy content of a fully charged tank.

In this paper, we present a new state calculation methodology based on the 1-dimensional (1-D) model originally proposed in [6], which was the first 1-D model to consider mixing and buoyancy dynamics using a smooth and continuous function. This model however was only validated against one tank topology and thus in a limited case study, which makes it unclear whether it works in tanks with other topologies and capacity or not. Besides the state estimation methodology, we also extend the work of [6] by integrating the different components of the model into a single dynamical equation making it easier to deploy under different contexts. This is needed as the original model approximated buoyancy differently depending on the type of charging and discharging used. To further improve upon the work of [6], we also extend and validate the model so that it can be applied to regular stratified storage tanks. This is important as the original model was conceived in the context of large seasonal storage systems where stratification effects are well-defined and only validated against a seasonal storage tank.

This paper is structured as follows. Section 2 focuses on the related work. The motivation and contributions of this work are presented in Section 3. The dynamical model is explained in Section 4 as well as the dynamics inside the tanks and the aggregation into a single model, including the corresponding formulas. The state estimation model is depicted in Section 5. Section 6 presents the case studies and gives more information on the tanks and implementation of the proposed approach. Results are discussed in Section 7 and the accuracy of the state estimation is assessed against sets of data collected during real experiments. Section 7 includes therefore three different phases: fitting phase during which parameters are estimated, state estimation during which temperature distribution is calculated and cross validation during which a different set of conditions is used to validate the model. Conclusions are finally drawn in Section 8.

2. Related work

The development of models that can estimate temperature inside stratified storage tanks has been the focus of several works. Han et al. [3], Njoku et al. [7] and Baeten et al. [8] provide an overview of the different types of models for stratified storage tanks, including 1-, 2- and 3-D approaches. In the context of this work, we focus on 1-D models as they are the most suitable option for optimization, e.g. temperature stratification and state of charge estimation, control processes, and long-term simulations of the behavior of thermal storage tanks, mainly due to the ability to simulate and give results in a short time span, which is key for optimization in almost real-time.

2.1. Overview

1-D models are vastly used in the literature and typically divide storage tanks into N layers and then model each layer with a partial differential equation (PDE) based on the heat transfer equation. Each layer is characterized by its temperature which is influenced by the input flow and corresponding temperature or by external input heat.

One of the drawbacks pointed out to most of the 1-D models is their inability to adequately reproduce situations where the stratification-by-cooling phenomenon, i.e. buoyancy, due to physical movement of water in two dimensions occurs. In particular, most of the existing models cannot deal with inversion when a layer is at a lower temperature than the layer immediately below [9–12]. In order to capture this phenomenon and adequately mix the given layers, some 1-D models implement extra computational artifices so that, at each time step, the distribution of temperatures is analyzed and, in case of colder layers above warmer layers, the mixing or interchange of the layers is done in a post-processing step [6,8]. Such artifices make the models non-smooth and their application in optimization problems very limited.

2-D models allow examining the outline of the mixing process [13] but are more complex computationally and thus not a first choice for control and optimization processes or long-term simulations of the behavior of thermal energy storage tanks.

3-D computational fluid dynamics (CFD) models are more accurate since they allow replicating as much as possible the dynamics happening inside the tank with the minimum level of simplifications [14,15]. They have however the same limitation as 2-D models: computational effort is quite high, narrowing their application in control and optimization problems.

In the background of 2 and 3-D models, as in 1-D models, differential equations are usually used. All three types of models allow predicting water temperature distribution inside storage tanks. Some specificities of each model are further presented in the following subsections.

2.2. 1-D models

This subsection intends to give an overview of models typically used to calculate the temperature distribution inside thermal storage tanks briefly presenting the main characteristics and drawbacks.

Baeten et al. [8] presented a 1-D model which is distinguishable from the typical 1-D models since it incorporates buoyancy and mixing due to direct charging and direct discharging. Missing model parameters were derived from CFD simulations and correlated with the suitable non-dimensional parameters and the model was validated using independent sets of charging and discharging. Although the authors state that the proposed model can be used in valid over a range of storage tank sizes and topologies, it is a non-smooth model due to the use of min and max functions which has limitations concerning its application in optimization problems.

De Césaro Oliveski et al. [13] performed a comparison between a 1-D model and a 2-D model. The 1-D model has some computational artifices to deal with temperature inversion and the 2-D model in cylindrical coordinates uses the finite volume method for which a turbulence model was added in mixed convection regime. The comparison of both models showed that both approaches give reliable results but also showed that the 1-D model does not produce so good results when thermal losses increase due to natural cooling and when the differences increase with time. Nevertheless, authors concluded that for long-term simulations, the 1-D model is faster and results are satisfactory. If more detailed information is needed and the understanding of thermal phenomena happening in the inside of the stratified storage tanks is one of the objectives, then 2-D models are more suitable.

Nelson et al. [9] and Spur et al. [10] did a comparison between the simplified 1-D model and CFD simulations and concluded that the 1-D model performs well for charging at low flow and constant temperature and flow, even without applying modifications for inflow mixing. Nelson et al. [9] focused on a tank with direct charging and discharging and can be used both for hot and chilled water while [10] validated their model in a residential storage tank with an heat exchanger (indirect charging).

Neupauer and Kupiec [16] based their work on a mathematical model for the heat transfer which considers heat losses to the environment through the walls, bottom and top of the stratified storage tank. The model was validated experimentally using different model parameters for different initial temperatures and assessed the changes

over time. The considered storage tank was placed vertically and had the typical cylindrical shape. Temperatures were assumed to be uniform within the same layer. Their results show that simulated temperature profiles shift towards lower temperatures with time, that the changes in the upper part of the tank occur faster than at the bottom part and that small discrepancies occur in the middle of the tank in the initial stage of cooling down.

A model based on 1-D transient heat balance equations was presented in [17] and was used to calculate the temperature distribution of the water inside a pressurized storage tank with indirect charge and indirect discharge. The tank had two heat exchangers with variable flow rates. The considered model includes the effect caused by these variable flow rates and, besides giving information about the temperature stratification inside the tank, it also computes the temperature of heat transfer fluids inside the heat exchangers and tests the impact of changing the vertical length and location of the heat exchangers on the water stored inside the tank.

Kreuzinger et al. [18] used two different approaches to estimate the spatial temperature in a stratified domestic hot water storage tank with indirect charging. The selected approaches were distributed parameter observer and Unscented Kalman Filter (UKF). They are based on a "finite state automaton interacting with an underlying thermal heat conduction–convection system described by a quasi-linear" PDE. Their comparison was done based on applicability, convergence behavior and number of function evaluations. The distributed parameter observer required the determination of appropriate interpolation functions between the temperature sensors and the adequate choice of the correction gain, which could be based on a physical interpretation, so that convergence was assured. The UKF is robust against an inadequate choice of the tuning parameters but convergence speed might be a bit low depending on the estimator. Both the approaches are able to estimate the temperature along the vertical axis of the tank but the distributed parameter observer outperforms the UKF in terms of number of necessary calculations and cost of computation.

More recently, Lago et al. [6] proposed the first 1-D model that overcame the limitations of existing models as it integrated, for the first time, the mixing and buoyancy effects using a smooth and continuous function and avoiding numerical artifices. They showed that the model was not only accurate, but had low computational requirements and could be efficiently integrated in optimization and control problems. Despite the novelty, the study had several limitations: (i) it was only proposed in the context of seasonal storage systems where stratification is a well-behaved effect, (ii) it was not validated for direct charge/discharge where the flow of water can cause bad-behaved buoyancy effects and (iii) it approximated buoyancy with different terms depending on the type of charging and discharging used. It can be therefore argued that this validation used an easier topology because of limited mixing and buoyancy effects. Topologies with direct charging which cause the destruction of any existent stratification still need however to be validated and thus the necessity of extending and validating the proposed model.

2.3. Other models

It is important to note that although 1-D models based on PDE are the most common choice to calculate temperature distribution inside stratified storage tanks, other approaches can also be used, as the already mentioned 2-D and 3-D models. Besides those models, other approaches have been used, namely: artificial neural networks (ANN) [19] and Markov Chain models [20], among others.

[19] relied on an ANN scheme for modeling layer temperatures inside a storage tank based on measured data, namely on solar radiation, ambient temperature, mass flow rate of collector loop, loading and temperature of the layers in previous time steps. The proposed approach avoids therefore the use of differential equations. The model therein proposed was composed of two parts describing the loading periods and the periods in-between. This approach does not allow however variations in the temperature of the inlet temperature of discharge water. The need of pre-existing data for training the ANN model is pointed out as a disadvantage by some authors.

Mathieu & Callaway [20] use Markov Chain models for describing temperature evolution of populations of TCLs and a discrete time difference equation to model individual behavior.

3. Motivation and contribution

Estimating the temperature distribution of water inside storage devices is paramount to efficiently use them to reduce the intermittent nature of renewable sources and also to make this type of resource manageable in terms of optimization and control contributing to energy flexibility from a demand side perspective [21]. In the context of stratified tanks, using 1-D models is arguably the most accurate and efficient technique to estimate the temperature distribution: (i) unlike black box models like ANNs, they are highly accurate as they have no risk of modeling spurious effect due to a lack of data, i.e. they consider the actual thermal behavior of the tank; (ii) unlike 2-D and 3-D models, they are very efficient as they require low computational requirements. Thus, temperature distribution estimation via 1-D models is crucial to include stratified thermal energy storage tanks in control and optimization problems and optimize their economic profits [22, 23].

Despite their importance and wide application, the existing 1-D models in the literature typically have several drawbacks being the main problem that most of them are non-smooth and thus too slow for real-time application. While the model proposed by [6] is a smooth model, it has several drawbacks which prevents it from being directly used with other types of tanks, namely:

1. It was proposed in the context of large seasonal storage systems where stratification in the tank behaves nearly perfect. This means that the large volume of storage water inside the tank is kept stratified which makes buoyancy effects easier to model.
2. Its validation was done only using indirect charge and discharge. This means that, due to the tank topology, there is no flow entering and leaving the tank, contributing again for a better defined stratification. Therefore, it is unclear whether the proposed model would work for direct charge/discharge, which can cause the destruction of any existent stratification, as already argued. Such validation is important because, although indirect charge/discharge can easily maintain stratification, it is also less efficient due to the indirect transfer of heat.
3. The approximation used in the model to integrate buoyancy effects differs depending on the type of charging and discharging used.

Besides these issues, an additional problem with existing models is that they are often not tested in the context of state estimation (arguably their most important requirement), and even when tested in that context, only a single tank topology is typically considered, i.e. either direct charge/discharge or indirect charge/discharge. As a result, it is not clear how well they generalize to other tank topologies and tank sizes.

In this paper, we try to address these issues via four contributions:

1. We extend the 1-D model of [6] so that the model is given by a single dynamical equation independently of the type of topology used.
2. the temperature distribution estimation methodology for stratified storage tanks proposed considers both buoyancy and mixing effects.
3. We validate the mentioned model in regular tanks to show that the model can also be applied for small-sized tanks and not just for large seasonal storage systems where stratification is easily kept.

4. We show that the model can be also efficiently used for direct charge/discharge topologies where the water flow destroys stratification and introduces unpredictable buoyancy effects. The proposed temperature distribution estimation methodology is validated therefore against multiple tank topologies to overcome the limitation of the original study [6] where stratification was easily kept as no flow entered/left the tank.
5. We build and propose the most complete case study for modeling and estimating the temperature distribution in stratified storage tanks: the case study is based on three different tanks comprising multiple topologies:
   (a) tanks with direct charging and discharging
   (b) tanks with indirect charging and direct discharging
   (c) tanks with different tank placements, i.e. horizontal as well as vertical tanks.

4. Dynamical model

To derive the 1-D model, it is assumed that stratified heat storage tanks can be divided into N layers. In addition, it is assumed that each layer i is characterized by a state T_i representing the temperature of the layer. This state can be controlled by (i) the input flow $\dot{m}_i$ and its temperature T_i^{in} or (ii) by the external input heat $\dot{Q}_i$ in the layer. According to [6], defining by α, ρ, and c_p the fluid diffusivity, density, and specific heat, by A_i, P_i, and Δz_i the cross-sectional area, perimeter, and thickness of layer i, by k_i the thermal conductance of the isolation wall of layer i, and by T_∞ the ambient temperature (ground temperature if the vessel is underground), the evolution of the temperature of layer i can be defined by the following PDE:

$$\frac{\partial T_i}{\partial t} = \alpha \frac{\partial^2 T_i}{\partial z^2} + \frac{P_i k_i \left(T_\infty - T_i\right)}{\rho c_p A_i} + \frac{\dot{Q}_i}{\rho c_p A_i \Delta z_i} + \frac{\dot{m}_i \left(T_i^{\text{in}} - T_i\right)}{\rho A_i \Delta z_i} \tag{1}$$

If this PDE is discretized and integrated in time using a forward Euler scheme we can obtain a discretized equation that describes the evolution of the temperature T_i at layer i:

$$\begin{aligned} T_{k+1,i} = T_{k,i} + \Big(& \alpha \frac{T_{k,i+1} + T_{k,i-1} - 2T_{k,i}}{\Delta z_i^2} + \beta_i \left(T_\infty - T_{k,i}\right) \\ & + \frac{\lambda_i}{\Delta z_i} \dot{Q}_{k,i} + \frac{\phi}{\Delta z_i} \dot{m}_{k,i} \left(T_{k,i}^{\text{in}} - T_{k,i}\right) \Big) \Delta t \end{aligned} \tag{2}$$

where:

$$\beta_i = \frac{P_i k_i}{\rho c_p A_i}, \quad \lambda_i = \frac{1}{\rho c_p A_i}, \quad \phi = \frac{1}{\rho A_i}, \tag{3}$$

and where $T_{k,i}$ is the temperature of layer i at time step k, $\dot{Q}_{k,i}$, $\dot{m}_{k,i}$, and $T_{k,i}^{\text{in}}$ the control inputs of layer i at time step k, Δt the length of the time step, and Δz_i is the thickness of layer i. For the sake of completion, the different terms, parameters, and variables of the heat storage tank model are listed in Table 1.

4.1. Buoyancy effects

Buoyancy effects occur when, given two consecutive layers, the upper layer is at a lower temperature when compared against the layer immediately below. In this situation, the lower temperature layer sinks while the layer with higher temperature raises and mixing of the layers occurs. This is also linked to gravity and density difference, since cold water which has a higher density will sink while warmer water with lower density causes the water to move up [3,13].

In traditional 1-D models, the temperature of all layers is checked by means of a computational artifice to detect buoyancy effects. If buoyancy is detected, the temperature of the layers is mixed following a simple average rule. This leads to models that are non-smooth and continuous. In the model considered in this paper, this issue is solved with different mathematical approximations. The end result is a smooth and continuous model. Here we provide the main idea behind these mathematical approximations; for further details, we refer to [6].

4.2. Slow and fast buoyancy effects

Slow buoyancy effects are linked to processes which occur naturally, namely inversion of water due to heat losses: as the top layer has usually a large contact area with the atmosphere, it loses more heat than other layers, its temperature decreases faster, and inversion due to buoyancy occurs. The effects caused by slow buoyancy can be modeled [6] by:

$$\begin{aligned} T_{k+1,i} = T_{k,i} + \Big(& \alpha \frac{T_{k,i+1} + T_{k,i-1} - 2T_{k,i}}{\Delta z_i^2} + \beta_i \left(T_\infty - T_{k,i}\right) \\ & + \frac{\lambda_i}{\Delta z_i} \dot{Q}_{k,i} + \frac{\phi}{\Delta z_i} \dot{m}_{k,i} \left(T_{k,i}^{\text{in}} - T_{k,i}\right) \Big) \Delta t \\ & + \theta_{i,i-1} \frac{1}{\mu} \log\left(e^0 + e^{\mu(T_{k,i-1} - T_{k,i})}\right) \\ & - \theta_{i,i+1} \frac{1}{\mu} \log\left(e^0 + e^{\mu(T_{k,i} - T_{k,i+1})}\right), \end{aligned} \tag{4}$$

where:

$$\theta_{i,i-1} = \frac{A_{i-1} \Delta z_{i-1}}{A_i \Delta z_i + A_{i-1} \Delta z_{i-1}} \in [0, 1]. \tag{5}$$

Fast buoyancy effects are associated with charging and discharging. According to [6], to include fast buoyancy effects in the heat storage tank model, we first need to consider whether the heat storage tank is based on direct or indirect operation.

In the case of direct charging/discharging, the model looks as follows:

$$\begin{aligned} T_{k+1,i} = T_{k,i} + \Big(& \alpha \frac{T_{k,i+1} + T_{k,i-1} - 2T_{k,i}}{\Delta z_i^2} + \beta_i \left(T_\infty - T_{k,i}\right) \\ & + \frac{\lambda_i}{\Delta z_i} \dot{Q}_{k,i} + \frac{\phi}{\Delta z_i} \dot{m}'_{k,i} \Big) \Delta t \\ & + \theta_{i,i-1} \frac{1}{\mu} \log\left(e^0 + e^{\mu(T_{k,i-1} - T_{k,i})}\right) \\ & - \theta_{i,i+1} \frac{1}{\mu} \log\left(e^0 + e^{\mu(T_{k,i} - T_{k,i+1})}\right), \end{aligned} \tag{6}$$

where the expression for $\dot{m}'_{k,i}$ depends on whether the tank is being charged or discharged:

$$\dot{m}'_{k,i} = \begin{cases} \displaystyle\sum_{l=0}^{i} \dot{m}_{k,l} \frac{\left(T_{k,l}^{\text{in}} - T_{k,i}\right) S(T_{k,l}^{\text{in}} - T_{k,i})}{\displaystyle\sum_{j=l}^{N} S(T_{k,l}^{\text{in}} - T_{k,j})}, & \text{if charging,} \\ \displaystyle\sum_{l=i}^{N} \dot{m}_{k,l} \frac{\left(T_{k,i} - T_{k,l}^{\text{in}}\right) S(T_{k,i} - T_{k,l}^{\text{in}})}{\displaystyle\sum_{j=0}^{l} S(T_{k,j} - T_{k,l}^{\text{in}})}, & \text{if discharging.} \end{cases} \tag{7}$$

In the expression above, $S\left(T_1 - T_2\right)$ represents the *logistic* function and approximates the step function:

$$S\left(T_1 - T_2\right) = \frac{1}{1 + e^{-\mu(T_1 - T_2)}}, \tag{8}$$

where μ is a scaling parameter that indicates how sharp the logistic function is, i.e. the larger the μ the closer the logistic function is to the step function.

Similarly, in the case of indirect charging/discharging, the model can be derived as follows:

$$\begin{aligned} T_{k+1,i} = T_{k,i} + \Big(& \alpha \frac{T_{k,i+1} + T_{k,i-1} - 2T_{k,i}}{\Delta z_i^2} + \beta_i \left(T_\infty - T_{k,i}\right) \\ & + \frac{\lambda_i}{\Delta z_i} \dot{Q}'_{k,i} + \frac{\phi}{\Delta z_i} \dot{m}_{k,i} \left(T_{k,i}^{\text{in}} - T_{k,i}\right) \Big) \Delta t \\ & + \theta_{i,i-1} \frac{1}{\mu} \log\left(e^0 + e^{\mu(T_{k,i-1} - T_{k,i})}\right) \end{aligned} \tag{9}$$

Table 1
Parameters and variables of the heat storage tank model.

Parameter	Description
T_i [K]	Temperature of layer i
α [m^2/s]	Fluid diffusivity
ρ [kg/m^3]	Fluid density
c_p [J/(kg K)]	Specific heat
A_i [m^2]	Cross-sectional area of layer i
P_i [m]	Perimeter
Δz_i [m]	Thickness of layer i (assumed to be the same for all the layers)
k_i [W/(m^2 K)]	Thermal conductance of the isolation wall of layer i
T_∞ [K]	Ambient temperature
$\dot{Q}_i$ [J]	Indirect (dis)charging[b] – input heat
$\dot{m}_i$ [kg/s]	Direct (dis)charging[a] – input mass flow
T_i^{in} [K]	Temperature of water flowing into layer i. It refers to both the water from the inlet pipe if the layer i is connected to the inlet pipe and the water from layer $i-1/i+1$ if the tank is being discharged/charged.
λ [m K/J]	Coefficient of the input heat
β_i [1/s]	Coefficient of heat losses of layer i.

[a]Direct charging means that there is hot water entering at the top of the tank and colder water leaving at the bottom. Direct discharging means that hot water is leaving the tank at the top and cold water is entering the tank at the bottom.
[b]Indirect charging means that the tank receives heat by means of a heat exchanger. In the indirect discharging the tank releases heat also through a heat exchanger.

$$- \theta_{i,i+1} \frac{1}{\mu} \log\left(e^0 + e^{\mu(T_{k,i}-T_{k,i+1})}\right),$$

where again the new expression for the input heat flow $\dot{Q}'_{k,i}$ also depends on whether the tank is being charged or discharged:

$$\dot{Q}'_{k,i} = \begin{cases} \sum_{l=0}^{i} \dot{Q}_{k,l} \cdot \dfrac{S(T_{k,l}-T_{k,i})}{\sum_{j=l}^{N} S(T_{k,l}-T_{k,j})}, & \text{if charging,} \\ \sum_{l=i}^{N} \dot{Q}_{k,l} \cdot \dfrac{S(T_{k,l}-T_{k,i})}{\sum_{j=0}^{i} S(T_{k,l}-T_{k,j})}, & \text{if discharging.} \end{cases} \tag{10}$$

The two types of buoyancy effects can be included in the model according to the single model presented in 4.3, for both indirect and direct charging/discharging.

4.3. Single model

In this paper, we argue that the different expressions for describing buoyancy can be integrated into a single equation. In particular, from a mathematical perspective, integrating all five effects, i.e. slow buoyancy, direct charging, direct discharging, indirect charging and indirect discharging, into a single equation poses no problem. The resulting model would be:

$$\begin{aligned} T_{k+1,i} &= F_i(\mathbf{T}_k, \dot{\mathbf{Q}}_k, \dot{\mathbf{m}}_k, \Delta k, \boldsymbol{\varphi}, \mathbf{T}_k^{\text{in}}) \\ &= T_{k,i} + \Bigg(\alpha \frac{T_{k,i+1} + T_{k,i-1} - 2T_{k,i}}{\Delta z_i^2} + \beta_i \left(T_\infty - T_{k,i}\right) \\ &+ \frac{\phi}{\Delta z_i} \sum_{l=0}^{i} \dot{m}_{k,l} \frac{\left(T_{k,l}^{\text{in}} - T_{k,i}\right) S(T_{k,l}^{\text{in}} - T_{k,i})}{\sum_{j=l}^{N} S(T_{k,l}^{\text{in}} - T_{k,j})} \\ &+ \frac{\phi}{\Delta z_i} \sum_{l=i}^{N} \dot{m}_{k,l} \frac{\left(T_{k,i} - T_{k,l}^{\text{in}}\right) S(T_{k,i} - T_{k,l}^{\text{in}})}{\sum_{j=0}^{l} S(T_{k,j} - T_{k,l}^{\text{in}})} \\ &+ \sum_{l=0}^{i} \frac{\lambda_i \dot{Q}_{k,l}}{\Delta z_i} \frac{S(T_{k,l}-T_{k,i})}{\sum_{j=l}^{N} S(T_{k,l}-T_{k,j})} \\ &+ \sum_{l=i}^{N} \frac{\lambda_i \dot{Q}_{k,l}}{\Delta z_i} \frac{S(T_{k,l}-T_{k,i})}{\sum_{j=0}^{i} S(T_{k,l}-T_{k,j})} \Bigg) \Delta t \\ &+ \theta_{i,i-1} \frac{1}{\mu} \log\left(e^0 + e^{\mu(T_{k,i-1}-T_{k,i})}\right) \\ &- \theta_{i,i+1} \frac{1}{\mu} \log\left(e^0 + e^{\mu(T_{k,i}-T_{k,i+1})}\right) \end{aligned} \tag{11}$$

where $\mathbf{T}_k$ is the vector of temperatures at time step k, $\dot{\mathbf{Q}}_k$ the vector of indirect heat at time step k, $\dot{\mathbf{m}}_k$ the vector of input flows at time step k, $\mathbf{T}_k^{\text{in}}$ the vector of input temperatures at time step k, and $\boldsymbol{\varphi}$ the vector of parameters defining the model.

5. State estimation

Assuming that the 1-D model for the tank is available, the proposed methodology for state estimation is based on a simple moving horizon estimation (MHE) [24]. In detail, to estimate the state of the tank at the current time step t_0, i.e. T_0, we solve an optimization problem considering the last n_{m} measurements up to time step t_0 that maximizes the likelihood of observing these measurements, i.e. we apply maximum likelihood estimation in a receding horizon manner.

Assuming independent and identically distributed Gaussian noise in the sensor measurements, the optimization problem that is estimated at every time step is defined as:

$$\underset{\mathbf{T}_{t_0-n_{\text{m}}},\ldots,\mathbf{T}_0}{\text{minimize}} \sum_{j\in\psi} \|\bar{\mathbf{T}}_j - \mathbf{T}_j\|_2^2 \tag{12a}$$

subject to

$$\begin{aligned} T_{k+1,i} &= F_i(\mathbf{T}_k, \dot{\mathbf{Q}}_k, \dot{\mathbf{m}}_k, \Delta k, \boldsymbol{\varphi}, \mathbf{T}_k^{\text{in}}) \\ &\text{for } k = t_0 - n_{\text{m}}, \ldots, -1, \text{for } i = 1, \ldots, N \end{aligned} \tag{12b}$$

where ψ is the set of time indices when temperature measurements are available and $\overline{\mathbf{T}}_k$ is the vector of temperature measurement at time step k.

In this formulations, two assumptions are made: (i) the parameters $\boldsymbol{\varphi}$ of the model are known and (ii) the inputs of the model are error free. If the first assumption does not hold, one could first estimate the parameters of the model following a similar approach [6]. If the inputs of the model have measurement errors, one could integrate them in the MHE approach by considering a second term in the objective function penalizing the inputs w.r.t. the measured inputs.

6. Case study

Besides proposing the state estimation approach, a second aim of this paper is to validate the smooth and continuous model in two scenarios: (i) multiple tank topologies with a focus on direct charge and discharge, and (ii) small-sized tanks where stratification is easily destroyed and buoyancy effects are not well-behaved. In this section, we describe the systems used for validating this model and testing the state estimation approach as well as the methodology used for the validation.

6.1. Description of the tanks

We consider two different case studies:

- A small industrial site where an interior and construction company burns waste wood to heat their offices, workshop and painting room and then uses the remaining heat to produce electricity in an ORC (Organic Rankine Cycle) [25]. Then, the excess heat from the ORC is stored for later use in two vertically placed stratified water storage tanks, which respectively have a capacity of 20 and 50 m^3.
- A residential house where two thermal storage tanks sized 12 m^3 each are installed [26]. These tanks, horizontally placed underground, can store surplus energy generated by solar collectors during summer to be used during winter for heating purposes. There is also a domestic hot water tank sized 0.4 m^3 which is also used to store energy in the form of heat. However, this tank differs from the others as it is indirectly charged and it is much smaller.

Based on these two case studies, we consider three different tanks:

1. The 50 m^3 tank from the first case study. This tank, referred henceforth as Tank A, employs a direct charging and discharging topology. The tank is depicted in Fig. 1.
2. One of the two 12 m^3 tanks from the second case study. This tank, referred henceforth as Tank B, also employs a direct charging and discharging topology. The tank is depicted in Fig. 2.
3. The 0.4 m^3, i.e. 400 l, tank from the second case study. This tank, referred henceforth as Tank C, also employs an indirect charging with direct discharging topology. The tank is depicted in Fig. 3.

6.1.1. Tank topologies

By including these three tanks in the case study, we ensure that the model and the SoC approach are tested and evaluated in a range of different sizes and tank topologies. In particular, depending on the type of charging, the tanks used in the case studies can be divided into two groups:

1. Tanks with direct charging and discharging (Tanks A and B).
2. Tanks with indirect charging and direct discharging (Tank C).

6.1.2. Tank placements

Besides having different topology, the tanks also have different placements to ensure that the model and SoC approach are tested in multiple conditions. In detail, two of the tanks are placed in a vertical position and in a room (Tank A and C) and the third one (Tank B) is located in a horizontal position and underground (Fig. 2).

By having these different placements we ensure that the case study includes the different variations encountered in real-life conditions: different orientation of the tank and different surrounding environment.

6.1.3. Sensors and heat exchangers location

For each of the three tanks, Figs. 1 to 3 depict the location of the sensors, the inlet and outlet pipes, and the coils in each tank.

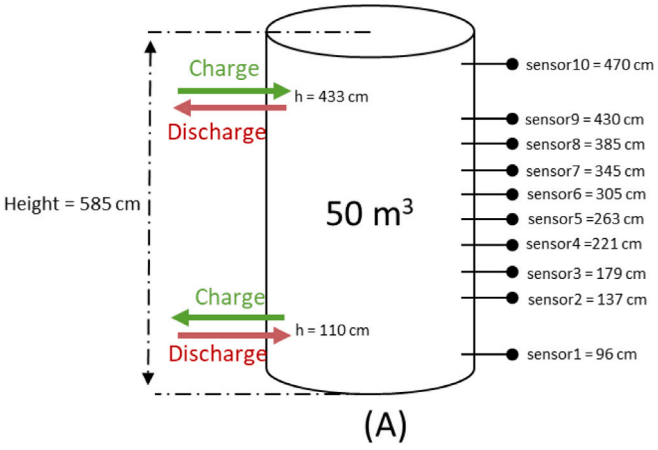

Fig. 1. Simplified representation of the Tank A, i.e. the 50 m^3 stratified thermal energy storage tank with direct charging and direct discharging.

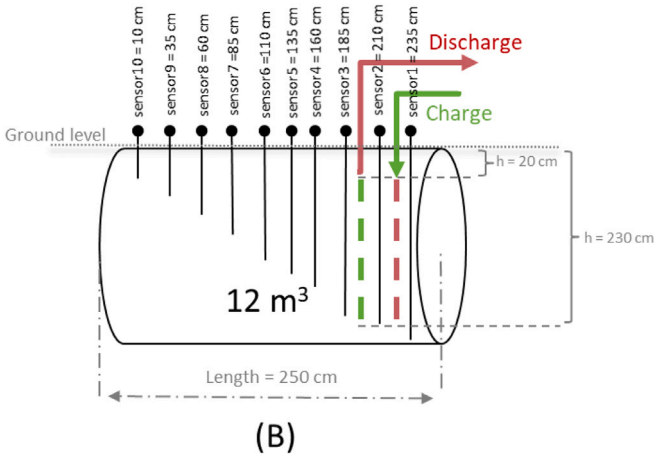

Fig. 2. Simplified representation of the Tank B, i.e. the 12 m^3 stratified thermal energy storage tank with direct charging and direct discharging.

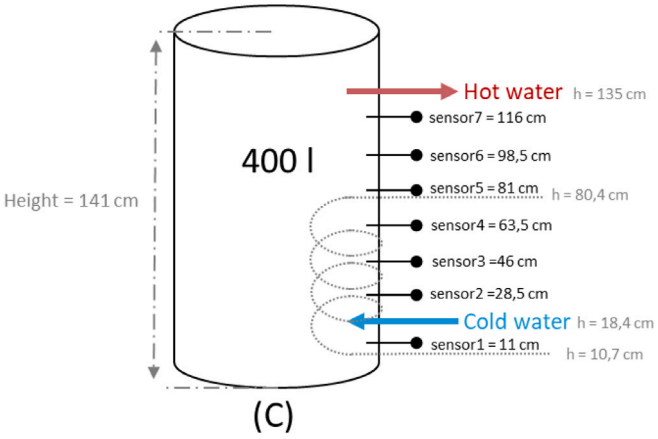

Fig. 3. Simplified representation of the Tank C, i.e. the 400 liters stratified thermal energy storage tank with indirect charging and direct discharging.

6.2. Data

The data used was collected during monitored tests of the EU funded H2020-STORY project [27]. For each tank, these data was divided between a *training* dataset used to estimate the parameters of the

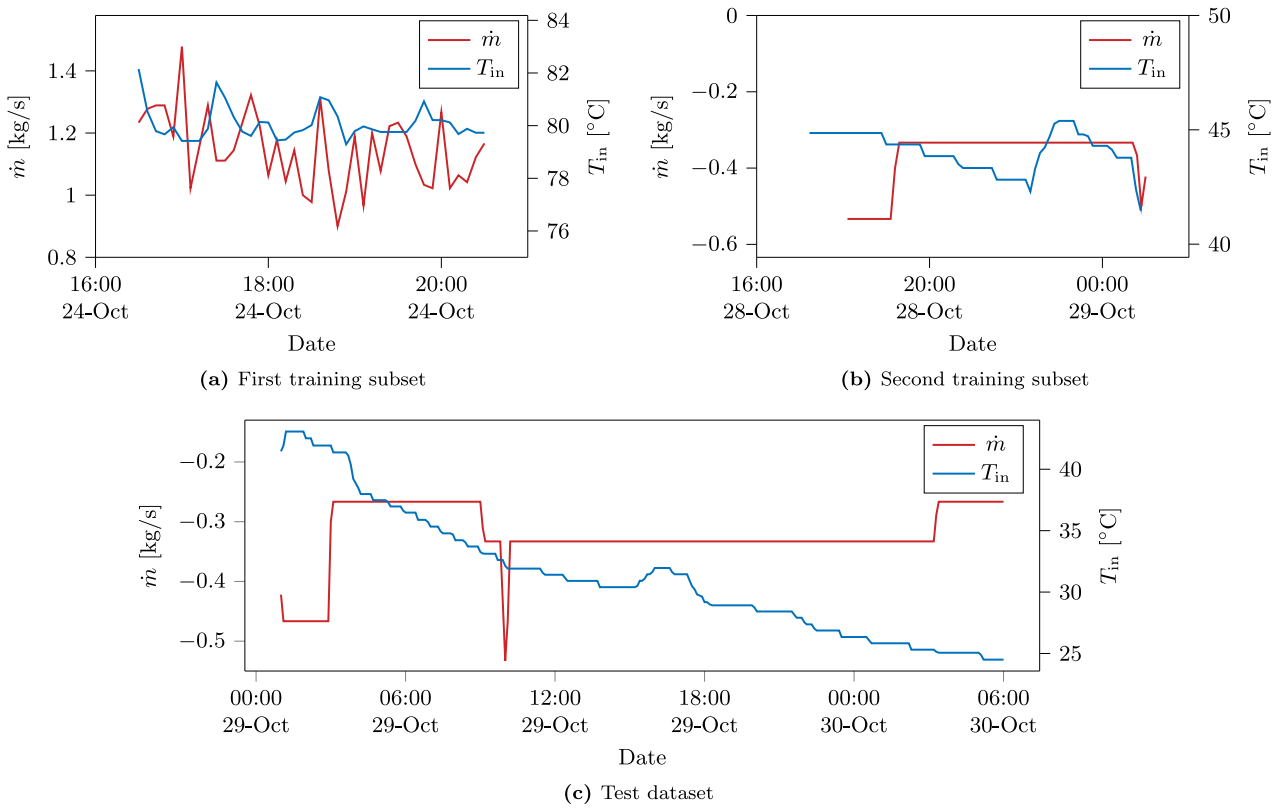

(a) First training subset

(b) Second training subset

(c) Test dataset

Fig. 4. Input controls, i.e. input flow $\dot{m}$ and input temperature T_{in}, for tank A in the training and test datasets. The training dataset is consist of data from two different dates: a first subset with 4 h of data on the 24/10/2017 and a second subset with 7 h of data on the 28/10/2017. The test dataset comprises 30 h of data from 29/10/2017–30/10/2017.

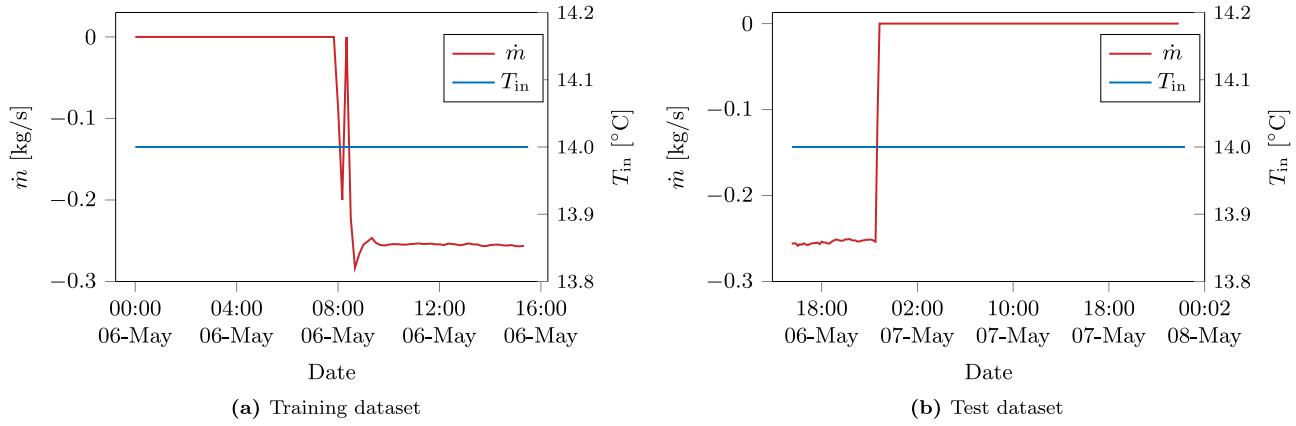

(a) Training dataset

(b) Test dataset

Fig. 5. Input controls, i.e. input flow $\dot{m}$ and input temperature T_{in}, for tank B in the training and test datasets.

model and test the SoC approach, and a *testing* dataset to evaluate the estimated model using an open-loop simulation.

The timestep, length, tank state, and the period of the data differed between the tanks. In particular, although we collected a large amount of data comprising multiple different tank states, we selected different states for each tank to ensure that the SoC approach was tested in multiple conditions; in particular, we considered the three different tank states: charging, discharging and idle.

For tank A the timestep from the measurements was 6 min both for the training and test sets and was collected at the end of October 2017. Both training and test datasets comprised charging and discharging states. The training dataset comprised two subsets: one comprising 4 h of data and a second one comprising 7 h of data; the test set comprised 30 h of data. The input controls for both training and test datasets are showed in Fig. 4.

For tank B the timestep was 10 min and was collected during May 2018. Both training and test datasets oscillate between idle and indirect discharging states. The training dataset began in an idle state and was followed by a discharging state; the test dataset displayed the opposite behavior. The inputs of both the training and test datasets are illustrated in Fig. 5.

For tank C the timestep was one minute and the data was collected in September 2017. Both training and test sets included simultaneously direct discharging and indirect charging. The input controls for the test set are displayed in Fig. 6.

6.3. Parameter estimation

To evaluate and validate the model in all conditions, i.e. small-sized tanks and direct charging and discharging, we perform a parameter

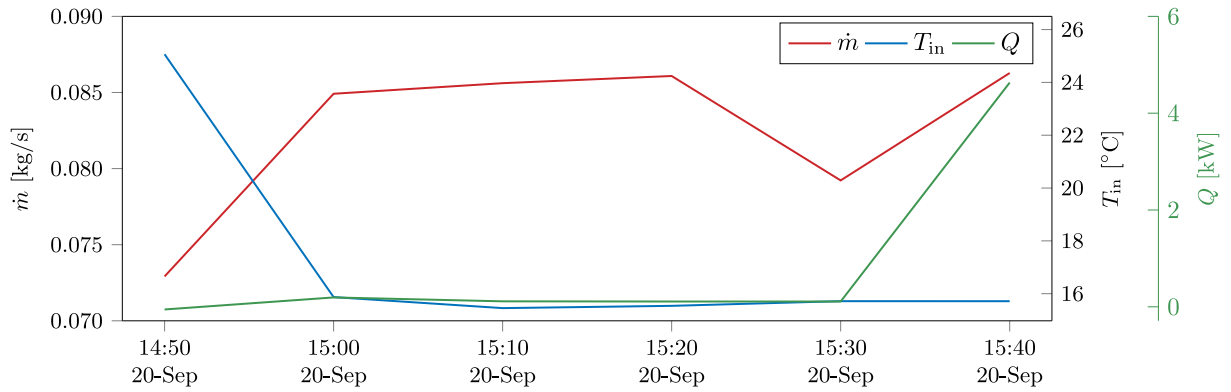

(a) Training dataset

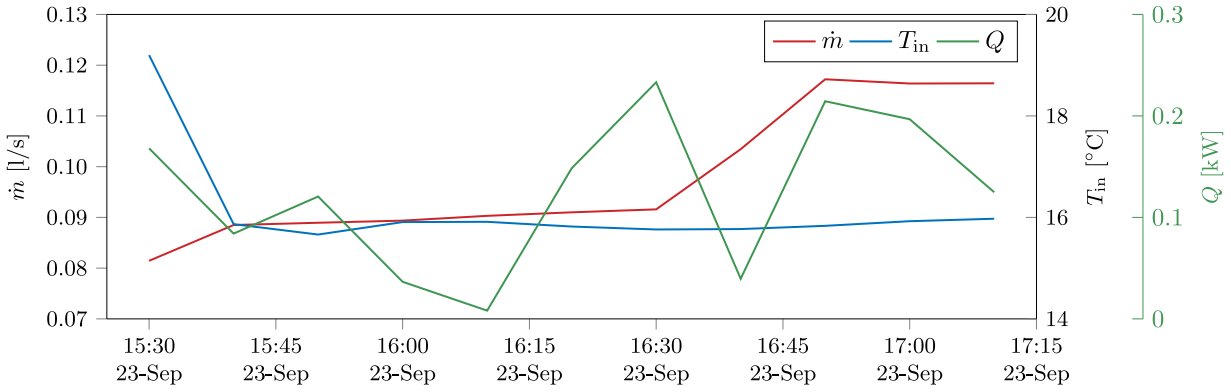

(b) Test dataset

Fig. 6. Input controls, i.e. input flow $\dot{m}$ and input temperature T_{in} for direct charging and output heat $\dot{Q}$ for indirect discharging, for tank C in the training and test datasets.

estimation task for each of the tanks. Then, based on the estimated parameters, we test the SoC approach. In this section, we describe the methodology for parameter estimation. In detail, as in [6], we identify the following parameters to be estimated:

- α: fluid diffusivity;
- β_i: coefficient of heat losses of the inner layers;
- β_1: coefficient of heat losses of the bottom layer;
- β_N: coefficient of heat losses of the top layer;
- λ: coefficient of the input heat;
- ϕ: coefficient of the input flow.

Then, given a set of $n_{\text{m}}+1$ temperature measurements $\{\overline{\mathbf{T}}_0, \dots, \overline{\mathbf{T}}_{n_{\text{m}}}\}$ distributed in time, the parameter estimation problem is defined as follows:

$$\underset{\boldsymbol{\varphi}, \mathbf{T}_0, \dots, \mathbf{T}_n}{\text{minimize}} \sum_{j \in \psi} \|\bar{\mathbf{T}}_j - \mathbf{T}_j\|_2^2 \tag{13a}$$

subject to

$$T_{k+1,i} = F_i(\mathbf{T}_k, \dot{\mathbf{Q}}_k, \dot{\mathbf{m}}_k, \Delta k, \boldsymbol{\varphi}, \mathbf{T}_k^{\text{in}}) \quad \begin{array}{l} \text{for } k = 0, \dots, n-1 \\ \text{for } i = 1, \dots, N, \end{array} \tag{13b}$$

It is important to note that in the above formulation we made two assumptions:

1. The time discretization for the parameter estimation might different from the time discretization where measurements available. To that end, we introduce the set ψ as the set of time indices when temperature measurements are available. In addition, we also distinguish between the number n_{m} of measurements and the number n of optimization variables.
2. As with the SoC approach, we assume that the inputs of the model $\{\dot{\mathbf{Q}}_1, \dots, \dot{\mathbf{Q}}_{n_{\text{m}}}\}$, $\{\dot{\mathbf{m}}_1, \dots, \dot{\mathbf{m}}_{n_{\text{m}}}\}$, and $\{\dot{\mathbf{T}}_1^{\text{in}}, \dots, \dot{\mathbf{T}}_{n_{\text{m}}}^{\text{in}}\}$ are available and error free. If the inputs of the model have measurement errors, one could integrate them in the optimization problem by considering a second term in the objective function penalizing the optimized inputs w.r.t. the measured inputs.

6.4. State estimation

To evaluate the SoC approach, we simply solve the optimization problem defined by (12a) using the training datset. In addition, to ensure that the SoC approach is tested in multiple conditions, we consider different the three different tank states: charging, discharging and idle.

For the sake of simplicity, we evaluate the SoC approach at a single time point, i.e. we perform a single iteration of the MHE technique. This first iteration using MHE shows that the model can be used for state estimation as long as a full set of temperature measurements is available.

6.5. Layer discretization

The three tanks considered were divided into a number of layers. The choice of the number of layers was tuned by experiment which showed that better results were achieved when a larger number of layers was considered for larger tanks. Taking that into account, the tanks were divided into the following number of layers:

- tank A – 15 layers (Fig. 7(a));
- tank B – 10 layers (Fig. 7(b));
- tank C – 7 layers (Fig. 8).

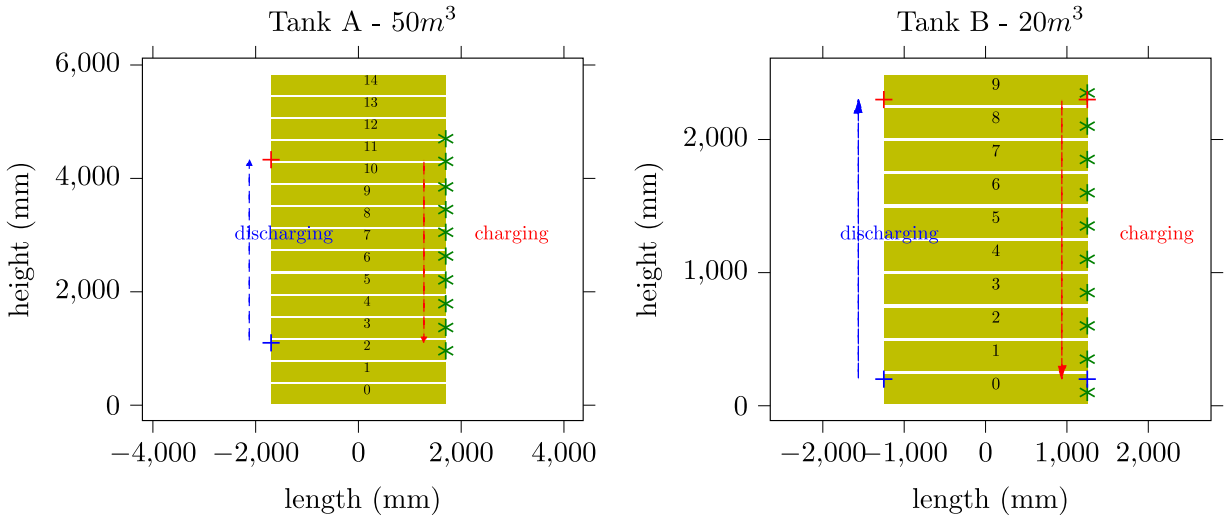

(a) Tank A **(b)** Tank B

Fig. 7. Representation of Tank A and B. Layers, sensors location (green symbol *), pipes represented by red symbol + and blue symbol +. The direction of the water flow according to the operation mode is represented by the arrows. The definition of inlet and outlet pipes is thus dependent on the mode. (For interpretation of the references to color in this figure legend, the reader is referred to the web version of this article.)

6.6. Evaluation metrics

For the validation of the model, we compare the temperature obtained through the use of the model in each timestep and height and the values observed. Based on those values the SoC model is evaluated in terms of the following errors:

- Average root mean square error (RMSE);
- Mean absolute error (MAE);
- Maximum absolute error (MaxAE).

The reasoning for evaluating three different errors is having a more realistic assessment of the accuracy of the methodology and not being biased by evaluating individual errors.

6.7. Software

Both the parameter estimation and the state estimation are modeled in Python using the mathematical modeling ramework CasADi [28] and solved using the interior point solver IPOPT [29]. The model was implemented using the discrete continuous dynamics described in Eq. (11), i.e. discretizing the PDE using Euler and including buoyancy. For the optimization, these dynamics were modeled using a multiple shooting approach [30]; this created a NLP with continuous dynamics that could be solved using a derivative-based optimization method like IPOPT.

7. Results and analysis

In this section, we present the obtained results. For the sake of simplicity, we divide this section in four parts. First, we present the results from the parameter estimation stage, during which full sets of measured data from completed experiments were used for fitting the model to data. Second, we present the results of the estimation. Third, we present the results of validating the model in a test dataset via simulation. Finally, we conclude the section with a brief discussion and analysis.

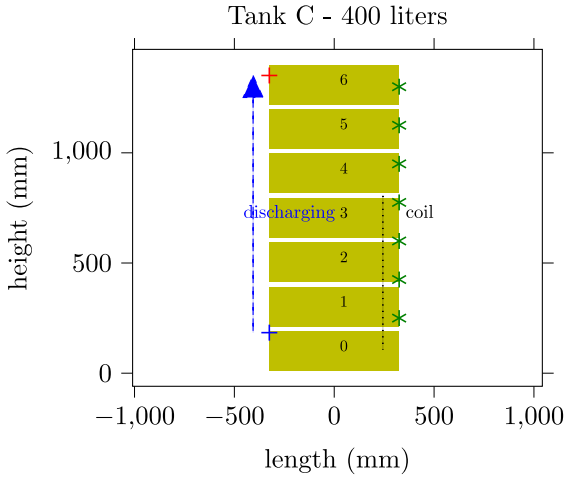

Fig. 8. Tank C — layers, sensors location (green symbol*), outlet pipe (red symbol +). Coil location represented in the picture by the black dotted line — it directly affects layers 0 to 3.

7.1. Parameter estimation

The estimated parameters are summarized in Table 2 and compared against the initial guess. From this table and analyzing the estimated parameters some unexpected values emerge, namely the 0 value for parameters β_i – coefficient of heat losses for the inner layers – for tanks B and C, β_N – coefficient of heat losses for the top layer – for tank B and λ – coefficient of the input heat – for Tank C. These 0 values, showing that non-physical solutions are found, are not expected since in reality there are heat losses for all the layers of the tanks. Although very strange, these results can be due (i) to the fact that we are solving a non-convex optimization problem and the obtained parameters are just local optimal, (ii) the impossibility of reliably estimating with this model all parameters from the set of measurements used, (iii) existent correlation between data and parameters or even (iv) over-parametrization of the model. Practical measures to solve this drawback are left for future research and include several options, namely, reduction of the parameter space and regularization using reference values [31].

Table 2
Estimated parameters.

Parameter	Initial guess			Estimated parameters		
	Tank A	Tank B	Tank C	Tank A	Tank B	Tank C
α	2.19E−06	2.19E−06	2.19E−06	1.36E−07	1.36E−07	1.36E−07
β_1	2.87E−06	4.30E−06	8.52E−06	3.19E−06	7.49E−06	1.44E−04
β_i	8.99E−07	1.22E−06	4.70E−06	4.45E−07	0	0
β_N	2.87E−06	4.30E−06	8.52E−06	6.12E−07	0	3.24E−06
λ	–	–	7.21E−07	–	–	0
ϕ	1.10E−04	2.03E−04	3.00E−03	1.29E−04	1.66E−04	3.10E−03

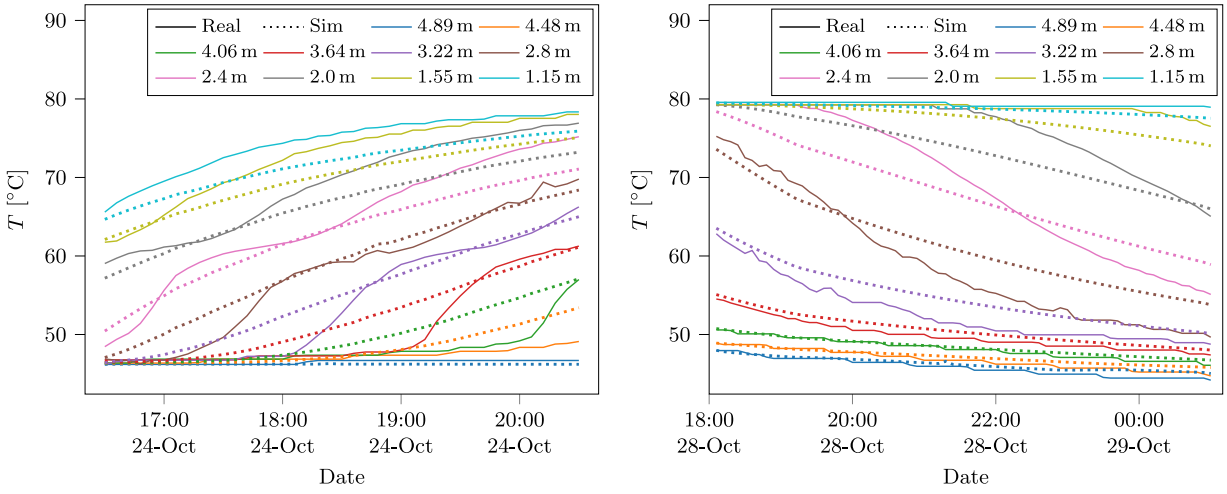

(a) First subset (b) Second subset

Fig. 9. Temperature evolution inside the tank A for the state estimation for different depths. The solid line represents the real measurements and the dotted lines the results from estimation. The left and right graphs respectively represent the temperature evolution for the first and second training subsets.

Table 3
State estimation errors.

	RMSE	MAE	MaxAE
Tank A	1.47	1.08	5.31
Tank B	2.58	1.56	12.78
Tank C	2.95	1.9	15.56

Table 4
Simulation estimation errors.

	RMSE	MAE	MaxAE
Tank A	1.67	1.38	9.77
Tank B	3.73	3.36	17.13
Tank C	4.8	2.97	15.79

7.2. State estimation

A summary of the results of the temperature distribution estimation is listed in Table 3 in terms of the RMSE, MAE, and MaxAE metrics.

Moreover, for tank A, the results of the temperature evolution is represented in Fig. 9. Although the maximum absolute error is 5.31 °C, the MAE is 1.08 °C, which is very acceptable. In particular, an average error below 1–2 °C is a very reasonable error for a 1-D model [6].

For tank B, the temperature evolution is illustrated in Fig. 10(a). The maximum absolute error has a value of 12.78 °C and occurs for the depth of 2.13 m which is located somewhere between sensors 1 and 2 and 17.5 cm above the inlet pipe. However, the average error is still low with a value of 1.56 °C. Considering that tank B is horizontal and has 1/3 of the volume of tank A, i.e. it has worse stratification properties than Tank A, the error is also reasonable.

For tank C, the temperature evolution is depicted in Fig. 10(b). The maximum absolute error is 15.6 °C but the average error is only 1.9 °C. Considering the extremely low volume of Tank C, i.e. 0.4 m^3, the average error for the last tank is also reasonable.

7.3. Model validation

To further validate that the model works not only for large seasonal storage systems with indirect charge/discharge, we simulate the estimated models for the three tanks in a test dataset. The results of the simulation are briefly summarized in Table 4.

For tank A, the simulation results are represented in Fig. 11. The maximum absolute error, as expected, is much higher than for the state estimation achieving a 9.8 °C maximum error. However, the average is still low at 1.38 °C. Such a small error seems to indicate that the estimated model is correct and that, as a result, the 1-D model also works for small tanks with direct charging and discharge.

For tank B, the simulation results are illustrated in Fig. 12. The maximum error was even higher than for tank A achieving 17,13 °C. This error appears on the top layer on the 7th May at 11:50 pm, which corresponds to a time when the idle mode was already in place for more than 24 h. As the simulated temperature is much lower than the real temperature, it is likely that this effect is due to the coefficient of heat loses being larger than reality; that would partially explain the fact that the estimated heat losses parameters of the middle layers (see Table 2) are 0 as they would have to do so to balance the large heat loses of the top layer. Although the simulated model does display a large error for the top layer, the error for the other layers is rather small, which again shows that even for a small tank, i.e. 12 m^3, the model works reasonably good.

Finally, for tank C, the simulation results are depicted in Fig. 13. It is important to note that, in comparison with the training dataset, the flow is higher and the amount of energy transferred is much lower (Fig. 6(b)). Since the flow is much higher and the energy transferred lower, the temperatures decrease much faster than during state estimation. Although the maximum error is 15.8 °C, the average error is below

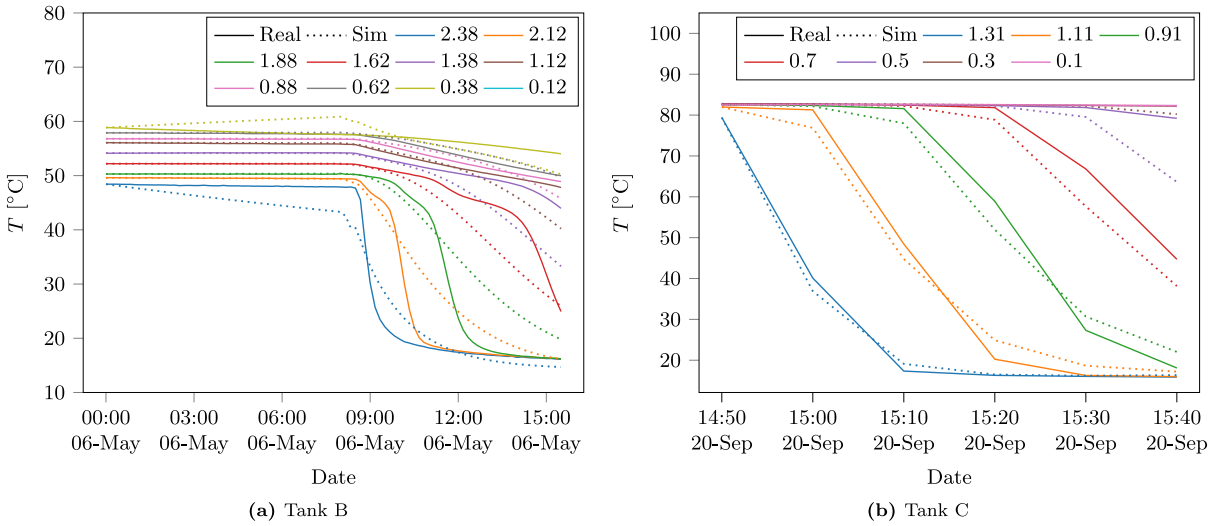

(a) Tank B (b) Tank C

Fig. 10. Temperature evolution inside the tank B for the state estimation for different depths. The solid line represents the real measurements and the dotted lines the results from estimation.

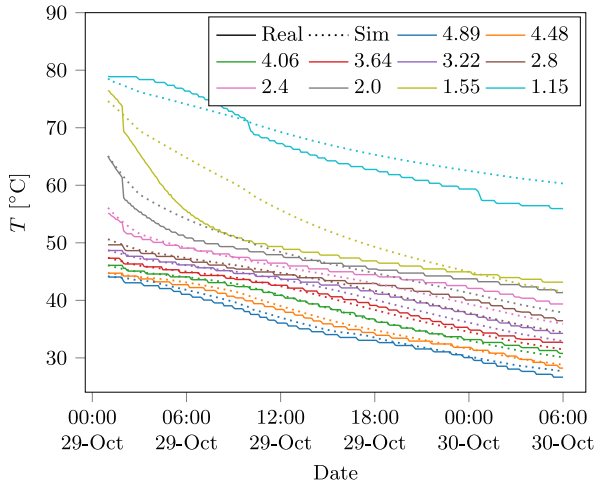

Fig. 11. Temperature evolution inside the tank A when simulating the test set. The solid line represents the real measurements and the dotted lines the results from simulation.

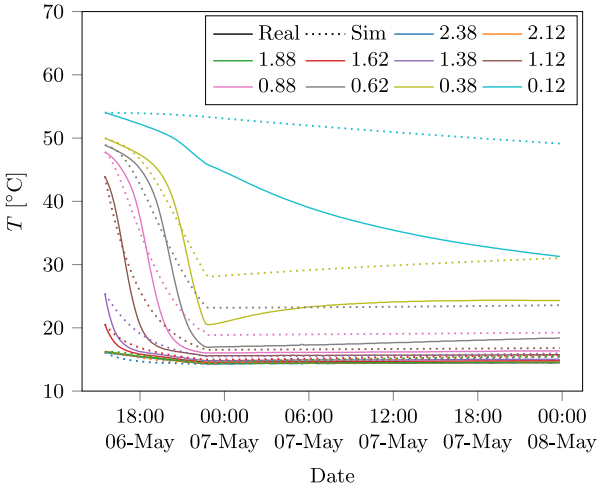

Fig. 12. Temperature evolution inside the tank B when simulating the test set. The solid line represents the real measurements and the dotted lines the results from simulation.

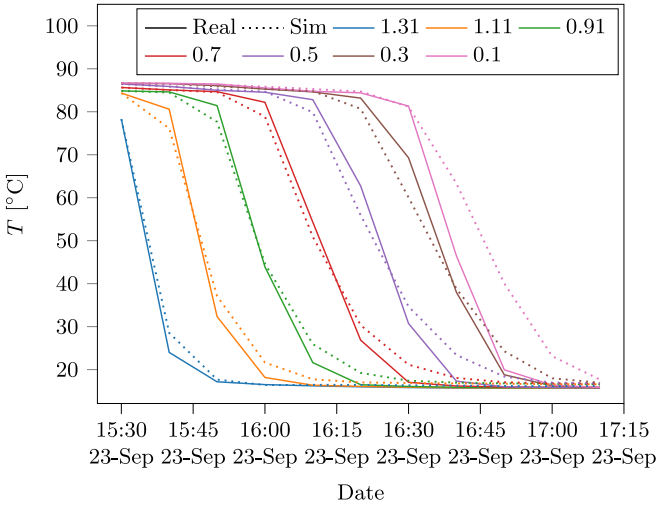

Fig. 13. Temperature evolution inside the tank C when simulating the test set. The solid line represents the real measurements and the dotted lines the results from simulation.

3 °C and the simulation appears to mimic quite good the temperature evolution. Considering the fact that tank C is really small, i.e. 0.4 m^3, these results further validate the validity of the model when small tanks with direct topologies are considered.

7.4. Discussion and analysis

Based on the results of temperature distribution estimation, it can be concluded that the proposed approach can be accurately used for state estimation. For all three tanks considering different sizes, topologies and placements, the average errors are always below 2 °C, which indicates that the model can accurately estimate the temperature distribution inside the tank.

Although some of the errors were high (>5 °C), they do not occur in all layers at the same point in time. So, if there is not an absolute need of very high accuracy when calculating temperature for each layer, in every single moment in time, then it is safe to assume that the presented approach performs reasonably well for different types of tanks, topologies, and sizes.

When it comes to the model itself, similar results can be observed when simulating the estimated models. Hence, the obtained results do indicate that the 1-D smooth and continuous model can also be applied to small tanks with direct charge/discharge where stratification effects are not as well-behaved; thus, the model is not limited to large seasonal tanks with indirect topologies.

If we compare the accuracy of the results presented in this section with the one displayed in [6], our accuracy results are slightly worse. However, as indicated multiple times through the paper, [6] only considered a large seasonal storage system with slower dynamics and with indirect charging. Such a system has simplified stratification dynamics effects as it avoids the thermal stratification destruction caused by direct charging. As a result, it is anyway expected to display lower average and maximum errors.

In short, taking all of this into account, it can be concluded that the proposed approach performs well and that the 1-D smooth and continuous model is not limited to large seasonal tanks with indirect topologies.

8. Conclusion

State estimation for stratified thermal energy storage play an important role to maximize the integration of renewables. Particularly, reliable estimation of the temperature evolution inside a storage tank is key for optimal energy storage, maximizing self-consumption, and in turn for optimal management of renewable energy production.

With that motivation, in this paper we proposed the first state estimation method for stratified thermal tanks that includes buoyancy and mixing effects. As these two dynamical behaviors dominate the dynamics of stratified tanks [6], the proposed method provides a state-of-the-art state estimation method for this type of storage systems. Besides this novel approach, we also improved the field of stratified storage tanks with two further contributions: first, we showed that the state-of-the-art 1-D smooth and continuous model for seasonal stratified storage tanks with indirect charge/discharge [6] can also be extended to small stratified tanks and to different topologies. Second, we proposed the most complete case study to date for modeling and estimating the temperature in stratified storage tanks.

To validate the proposed approach and the model extension, we considered real data from three different stratified storage tanks. First, we performed a model/parameter estimation for each one of the models. Then, we validated the estimated models using out-of-sample data and comparing the performance of the simulated models against the real data. Third, with the estimated models, we validated the SoC state estimation approach. For the sake of simplicity, this validation was limited to the case where the full set of temperatures was available (note that the observability and the possibility to reconstruct states when only a reduced set of temperature measurements is available still needs to be tested case by case). Finally, as both the state estimation approach and the simulation of the model displayed average mean errors below 2 °C, we could conclude that both model and state estimation approach are highly accurate.

In future work, we will focus on using this approach to cases where only a reduced set of temperature measurements is available. The aim of that work will be to study the observability and the possibility of reconstructing missing states with partial information. Additional studies regarding the estimator's convergence for a wider operating range and for long-term operation will also be conducted.

CRediT authorship contribution statement

Ana Soares: Software, Validation, Formal analysis, Investigation, Data curation, Writing – original draft, Revised submission, Writing – review & editing. **Juliano Camargo:** First review. **Jad Al-Koussa:** Investigation, First review. **Jan Diriken:** First review. **Johan Van Bael:** Supervision, Project administration, Responsible for the funding, First review. **Jesus Lago:** Software, Validation, Formal analysis, Investigation, Data curation, Writing – original draft, Revised submission, Writing – review & editing.

Declaration of competing interest

The authors declare that they have no known competing financial interests or personal relationships that could have appeared to influence the work reported in this paper.

Acknowledgments

The research leading to these results has received funding from the European Union's Horizon 2020 research and innovation programme under grant agreement no. 646426, Project Story – H2020-LCE-2014-3. Ana Soares also received funding from project grant UIDB/00308/2020.

References

[1] Z.J. Yu, G. Huang, F. Haghighat, H. Li, G. Zhang, Control strategies for integration of thermal energy storage into buildings: State-of-the-art review, Energy Build. 106 (2015) 203–215, http://dx.doi.org/10.1016/j.enbuild.2015.05.038.

[2] G. Reynders, R.A. Lopes, A. Marszal-Pomianowska, D. Aelenei, J. Martins, D. Saelens, Energy flexible buildings: An evaluation of definitions and quantification methodologies applied to thermal storage, Energy Build. 166 (2018) 372–390, http://dx.doi.org/10.1016/j.enbuild.2018.02.040.

[3] Y. Han, R. Wang, Y. Dai, Thermal stratification within the water tank, Renew. Sustain. Energy Rev. 13 (5) (2009) 1014–1026, http://dx.doi.org/10.1016/j.rser.2008.03.001.

[4] M. McPherson, S. Tahseen, Deploying storage assets to facilitate variable renewable energy integration: The impacts of grid flexibility, renewable penetration, and market structure, Energy 145 (2018) 856–870, http://dx.doi.org/10.1016/j.energy.2018.01.002.

[5] B.A. Frew, S. Becker, M.J. Dvorak, G.B. Andresen, M.Z. Jacobson, Flexibility mechanisms and pathways to a highly renewable US electricity future, Energy 101 (2016) 65–78, http://dx.doi.org/10.1016/j.energy.2016.01.079.

[6] J. Lago, F.D. Ridder, W. Mazairac, B.D. Schutter, A 1-dimensional continuous and smooth model for thermally stratified storage tanks including mixing and buoyancy, Appl. Energy 248 (2019) 640–655, http://dx.doi.org/10.1016/j.apenergy.2019.04.139.

[7] H.O. Njoku, O.V. Ekechukwu, S.O. Onyegegbu, Analysis of stratified thermal storage systems: An overview, Heat Mass Transf. 50 (7) (2014) 1017–1030, http://dx.doi.org/10.1007/s00231-014-1302-8.

[8] B. Baeten, T. Confrey, S. Pecceu, F. Rogiers, L. Helsen, A validated model for mixing and buoyancy in stratified hot water storage tanks for use in building energy simulations, Appl. Energy 172 (2016) 217–229, http://dx.doi.org/10.1016/j.apenergy.2016.03.118.

[9] J.E.B. Nelson, A.R. Balakrishnan, S.S. Murthy, Transient analysis of energy storage in a thermally stratified water tank, Int. J. Energy Res. 22 (10) (1998) 867–883, http://dx.doi.org/10.1002/(sici)1099-114x(199808)22:10<867::aid-er410>3.0.co;2-l.

[10] R. Spur, D. Fiala, D. Nevrala, D. Probert, Performances of modern domestic hot-water stores, Appl. Energy 83 (8) (2006) 893–910, http://dx.doi.org/10.1016/j.apenergy.2005.10.001.

[11] M. Rodríguez-Hidalgo, P. Rodríguez-Aumente, A. Lecuona, M. Legrand, R. Ventas, Domestic hot water consumption vs. solar thermal energy storage: The optimum size of the storage tank, Appl. Energy 97 (2012) 897–906, http://dx.doi.org/10.1016/j.apenergy.2011.12.088.

[12] A.A. Farooq, A. Afram, N. Schulz, F. Janabi-Sharifi, Grey-box modeling of a low pressure electric boiler for domestic hot water system, Appl. Therm. Eng. 84 (2015) 257–267, http://dx.doi.org/10.1016/j.applthermaleng.2015.03.050.

[13] R.D.C. Oliveski, A. Krenzinger, H.A. Vielmo, Comparison between models for the simulation of hot water storage tanks, Sol. Energy 75 (2) (2003) 121–134, http://dx.doi.org/10.1016/j.solener.2003.07.009.

[14] A. Pizzolato, F. Donato, V. Verda, M. Santarelli, CFD-based reduced model for the simulation of thermocline thermal energy storage systems, Appl. Therm. Eng. 76 (2015) 391–399, http://dx.doi.org/10.1016/j.applthermaleng.2014.11.029.

[15] W. Yaïci, M. Ghorab, E. Entchev, S. Hayden, Three-dimensional unsteady CFD simulations of a thermal storage tank performance for optimum design, Appl. Therm. Eng. 60 (1–2) (2013) 152–163, http://dx.doi.org/10.1016/j.applthermaleng.2013.07.001.

[16] K. Neupauer, K. Kupiec, Heat transfer during storage of hot liquid in the tank, Czasopismo Techniczne 4/2017 (2017) http://dx.doi.org/10.4467/2353737xct.17.045.6356.

[17] A. Rahman, A.D. Smith, N. Fumo, Performance modeling and parametric study of a stratified water thermal storage tank, Appl. Therm. Eng. 100 (2016) 668–679, http://dx.doi.org/10.1016/j.applthermaleng.2016.01.163.

[18] T. Kreuzinger, M. Bitzer, W. Marquardt, State estimation of a stratified storage tank, Control Eng. Pract. 16 (3) (2008) 308–320, http://dx.doi.org/10.1016/j.conengprac.2007.04.013.

[19] P. Géczy-Víg, I. Farkas, Neural network modelling of thermal stratification in a solar DHW storage, Sol. Energy 84 (5) (2010) 801–806, http://dx.doi.org/10.1016/j.solener.2010.02.003.

[20] J.L. Mathieu, D.S. Callaway, State estimation and control of heterogeneous thermostatically controlled loads for load following, in: 2012 45th Hawaii International Conference on System Sciences, IEEE, 2012, http://dx.doi.org/10.1109/hicss.2012.545.

[21] J.P. Iria, F.J. Soares, M.A. Matos, Trading small prosumers flexibility in the day-ahead energy market, IEEE Power Energy Soc. Gener. Meet. 2018-Janua (3) (2018) 1–5, http://dx.doi.org/10.1109/PESGM.2017.8274488.

[22] J. Lago, E. Sogancioglu, G. Suryanarayana, F.D. Ridder, B.D. Schutter, Building day-ahead bidding functions for seasonal storage systems: A reinforcement learning approach, IFAC-PapersOnLine 52 (4) (2019) 488–493, http://dx.doi.org/10.1016/j.ifacol.2019.08.258.

[23] J. Lago, G. Suryanarayana, E. Sogancioglu, B. De Schutter, Optimal control strategies for seasonal thermal energy storage systems with market interaction, IEEE Trans. Control Syst. Technol. (2020) http://dx.doi.org/10.1109/TCST.2020.3016077.

[24] J.D. Hedengren, R.A. Shishavan, K.M. Powell, T.F. Edgar, Nonlinear modeling, estimation and predictive control in APMonitor, Comput. Chem. Eng. 70 (2014) 133–148, http://dx.doi.org/10.1016/j.compchemeng.2014.04.013.

[25] STORY: The added value of storage in the distribution grid. Case study 6. URL http://horizon2020-story.eu/story_case_study/case-study-6/.

[26] STORY: The added value of storage in the distribution grid. Case study 1. URL http://horizon2020-story.eu/story_case_study/case-study-1/.

[27] STORY: The added value of storage in the distribution grid. URL http://horizon2020-story.eu/.

[28] J.A.E. Andersson, J. Gillis, G. Horn, J.B. Rawlings, M. Diehl, CasADi: a software framework for nonlinear optimization and optimal control, Math. Program. Comput. 11 (1) (2018) 1–36, http://dx.doi.org/10.1007/s12532-018-0139-4.

[29] A. Wächter, L.T. Biegler, On the implementation of an interior-point filter line-search algorithm for large-scale nonlinear programming, Math. Program. 106 (1) (2005) 25–57, http://dx.doi.org/10.1007/s10107-004-0559-y.

[30] H.G. Bock, K.J. Plitt, Multiple shooting algorithm for direct solution of optimal control problems., IFAC Proc. Ser. 17 (2) (1985) 1603–1608, http://dx.doi.org/10.1016/s1474-6670(17)61205-9.

[31] C.D.C. López, T. Barz, S. Körkel, G. Wozny, Nonlinear ill-posed problem analysis in model-based parameter estimation and experimental design, Comput. Chem. Eng. 77 (2015) 24–42, http://dx.doi.org/10.1016/j.compchemeng.2015.03.002, URL http://dx.doi.org/10.1016/j.compchemeng.2015.03.002https://linkinghub.elsevier.com/retrieve/pii/S0098135415000733.